Journal of Alloys and Compounds 503 (2010) 1–5

Contents lists available at ScienceDirect

Journal of Alloys and Compounds

journal homepage: www.elsevier.com/locate/jallcom

Structural and superconducting properties of YBaCuO superconductors at different atomic compositions

Ugur Topal [a,*], Mustafa Akdogan [b,1]

[a] TUBITAK-UME (National Metrology Institute), Magnetism Lab., P.K. 54, 41470 Gebze-Kocaeli, Turkey
[b] Department of Physics, Abant Izzet Baysal University, 14280 Bolu, Turkey

ARTICLE INFO

Article history:
Received 20 July 2009
Received in revised form 14 April 2010
Accepted 23 April 2010
Available online 6 May 2010

PACS:
74.25.Ha
74.25.Sv
74.62.Bf
74.72.Bk

Keywords:
YBaCuO
Superconductivity
Critical current

ABSTRACT

Mixing of Y_2O_3, $BaCO_3$ and CuO in proper amounts to yield a net composition of $YBaCu_2O_x$ reveals superconductivity above 90 K without the requirement of any post-annealing under oxygen flow. Advantage of this starting composition is observed as the samples take sufficient amount of oxygen during calcination process. We found that oxygenation does not change the crystal structure and the transition temperature but it seems to be effective for improvement of the superconducting properties of intergrain regions. The J_c values of as-sintered samples, which were calculated from the M–H curves, approach to the order of 10^6 A/cm^2 at 10 K. Oxygenated samples even take J_c values higher than 10^6 A/cm^2, which is mainly due to the improvement of intergrain regions.

1. Introduction

It is well known that the superconducting cuprates are highly oxidized compounds (the original $La_{1.85}Sr_{0.15}CuO_4$ superconductor has an average Cu valency of 2.15, while in $YBa_2Cu_3O_7$, the value is 2.33) and tend to lose oxygen during synthesis at high calcination temperature [1]. Among the cuprate superconductors, RE-Ba–Cu–O (RE: Nd, Sm, Y, Gd, etc.) has many potential applications because of its ability to work at liquid nitrogen temperature, but it also suffers from the problem of oxygen loss as much due to the requirement of high calcination temperatures in order to obtain desired phases.

Particularly in Y–Ba–Cu–O systems, oxygen content has crucial importance for controlling structure and superconducting state properties. Contrary to the high stability of the oxygen concentration in Y-124 system ($YBa_2Cu_4O_8$), in the Y–Ba–Cu–O HTSC family, Y-247 ($Y_2Ba_4Cu_7O_{14+x}$) and well known Y-123 ($YBa_2Cu_3O_{7-x}$) may lose oxygen easily and thus variations on their superconducting properties may be observed. For instance, as it is well known, Y-123 has a variable oxygen stoichiometry $0 \leq x \leq 1$ due to labile oxygen in the chain layer [2]. For these values of x, transition temperature was reported as changing from 93 K down to 0 K [3]. Besides, its structure undergoes a transition from tetragonal to orthorhombic phase around $x = 0.5$ [4]. In order to obtain high stability of oxygen concentration in Y-123 and Y-247 systems, many techniques have been performed and studies have been done up to now [5–11]. Processing in high-pressure oxygen gas may be given as an example [10,11].

In the present study, we succeeded to synthesize a superconducting Y–Ba–Cu–O compound with a transition temperature T_c of 90 K (even higher) without the necessity of any thermal treatment under oxygen. For comparison, the samples were oxidized under high oxygen flow rate and no variation on T_c was observed. To ensure the reproducibility, synthesis procedure was repeated many times for different samples and the same structural and superconducting properties could be obtained. In this paper, we share our findings with the superconductivity community.

2. Experimental part

The samples used in this study were synthesized as follows. High purity powders of Y_2O_3, $BaCO_3$ and CuO were weighted in proper amounts to form a nominal composition at $YBaCu_2O_x$. It is important to point that this is the key point which makes our results different from those in literature. Then the powders were thoroughly mixed using an agate mortar and pressed into disc-shaped pellets under pressures of 2000 kg/cm^2. The pellets were calcined at different temperatures between 900 and 1000 °C to find optimal calcination temperature for 20 h in a controllable box

* Corresponding author. Tel.: +90 2626795000; fax: +90 2626795001.
E-mail addresses: ugur.topal@ume.tubitak.gov.tr (U. Topal), akdogan_m@ibu.edu.tr (M. Akdogan).
[1] Tel.: +90 374 253 4506.

0925-8388/$ – see front matter © 2010 Elsevier B.V. All rights reserved.
doi:10.1016/j.jallcom.2010.04.224

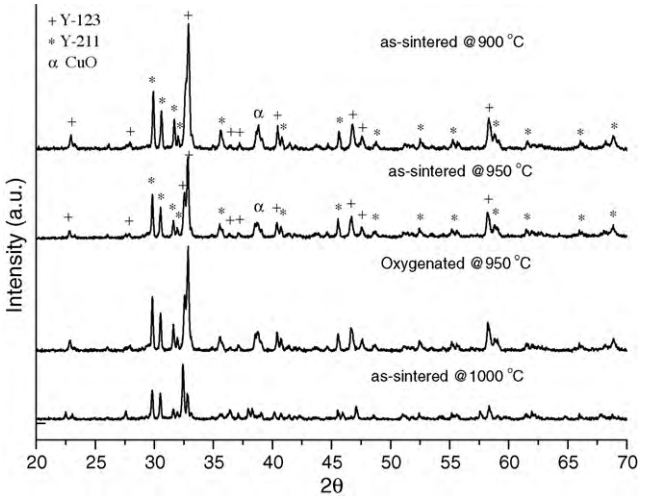

Fig. 1. The X-ray diffraction patterns of the oxygenated and as-sintered Y–Ba–Cu–O superconductors calcined at different temperatures.

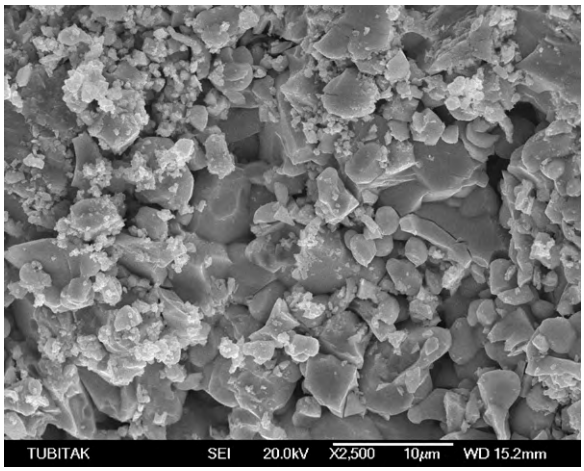

Fig. 2. Scanning electron microscopy (SEM) image of the oxygenated sample (calcined @950 °C).

furnace. Samples were regrinded, pelletized at same pressure and calcined again at the same temperature. One sample was left for the measurements (called as-sintered) and the other one was oxygenated under oxygen flow by slow cooling (50 °C/h) from the calcination temperature (900–1000 °C) to 450 °C, holding at this temperature for 2 days and then slow cooling again to 25 °C with 50 °C/h (called the oxygenated). This fabrication process was repeated several times to ensure the reproducibility of samples.

Structural analysis was done by Shimadzu XRD-6000 diffractometer (CuKα). The microstructural analysis was carried out using a scanning electron microscopy (JEOL 6335F Field Emission Gun). The specimens were cut into small regular pieces for magnetic measurements. The M–H loops and the M–T measurements were done in a Quantum Design MPMS-5 SQUID magnetometer. Electrical measurements were carried out using four-probe technique.

3. Results and discussions

Fig. 1 shows the X-ray patterns of the oxygenated (calcined @950 °C) and as-sintered (calcined @900, 950, 1000 °C) samples. It is seen that all samples contain large amounts of Y-211 phase (Y_2BaCuO_5) and small amounts of CuO phase. Y-211 content in all studied samples was observed to be almost constant and determined as ~50% with standard deviation of 4%. In order to check the reproducibility of samples with the same Y-211 content, 3 different samples, which were fabricated at different times, were also analyzed by X-ray diffractometry and the results were found to be consistent with those reported above (within the limits of standard deviation). Note that, as it was reported before, Y-211 phase behaves like pinning centers and thus their presence in Y-123 superconductors can be effective for the increase of critical current density J_c [12,13]. In addition, self-production of these impurity phases may be useful to obtain high J_c values in Y-123 system if the melt-texturing techniques are followed [14]. As seen from the X-ray graphs of both the oxygenated and as-sintered YBCO samples, which were calcined at 950 °C, there is no distinguishable difference between the patterns of these samples, such as sharpness, peak positions, etc. For instance, width of the most intense peak at half height ($2\theta = 32.84°$) of as-sintered and oxygenated samples were determined to be 0.20° and 0.21°, respectively. It means oxygen has not much influence on the crystallographic structure of these samples. It must be noted that characteristic diffraction peaks of Y-123 phase is seen in the diffraction pattern of as-sintered and oxygenated samples.

Scanning electron microscopy (SEM) image of the oxygenated sample (calcined @950 °C) is seen in Fig. 2. The image reveals that grain dimensions are less than 10 μm. Table 1 gives the results of elemental analysis made using scanning electron microscopy (SEM-EDS) and results re-evaluated after subtraction of the contribution of impurity phases Y_2BaCuO_5 and CuO. As seen, atomic ratios of elements after extracting the contribution of impurity phases differs from well known $YBa_2Cu_3O_7$ superconductors, on which atomic ratios of Y:Ba:Cu:O = 7.69:15.38:23.07:53.83 is expected.

Table 1
Atomic ratios of the elements obtained by using scanning electron microscopy for the oxygenated samples: original sample, results re-evaluated after subtraction of the contribution of impurity phase.

Element	Oxygenated sample	
	Original (with impurities) Atomic%	Re-evaluated (without impurities) Atomic%
Y	12.26	8.72
Ba	18.39	21.79
Cu	31.76	39.40
O	37.58	30.08

Fig. 3 shows temperature dependence of the diamagnetic shielding signals and Meissner signals for as-sintered and oxygenated samples. The diamagnetic shielding signal (zfc) was measured by cooling the sample in zero fields, and then applying a small field at the lowest measurement temperature. The Meissner signal (fc) was obtained by subsequently cooling the sample in the same field from above T_c. As seen from Fig. 3a, both the diamagnetic and Meissner signals increase by just 7% in magnitude with the oxygenation. On the other hand, superconducting transition T_c (on) starts at same temperature. T_c (on) is 90 K for both as-sintered and oxygenated samples. Shielding superconducting fraction (zfc) at 50 K is estimated to be ~35% of perfect diamagnetism for as-sintered sample in 50 Oe (see Fig. 3a). It is ~38% of perfect diamagnetism in the oxygenated one. Taking the volume fraction of non-superconducting Y-211 phase (~50% of Y-123 matrix) and large demagnetization factor due to the geometry into account (note that magnetic field was applied perpendicular to the 1.5 mm × 2.4 mm surface of the sample having dimensions of 1.5 mm × 2.4 mm × 1.8 mm), these fractions seem reasonable. Trapped fields at 77 K, which was determined from the difference of the diamagnetic and Meissner signals, are almost same in both samples. The trapped field increases by 12% in magnitude with the oxygenation. That is, concentration of effective pinning centers at 77 K increase but not much with the oxygenation. Superconducting transition widths of as-sintered and oxygenated samples, which were determined from 90% and 10% of diamagnetic signals, are about 14 and 8 K, respectively.

It is well known that carrier density, which determines the T_c (on) values, is quite dependent on the stoichiometry of the materi-

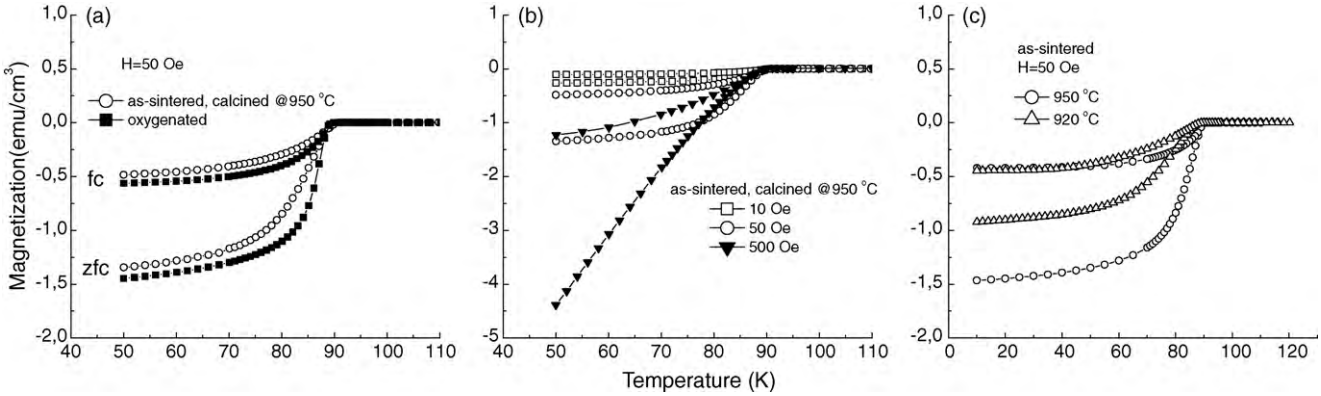

Fig. 3. The M–T curves of as-sintered and oxygenated samples.

als studied [15,16]. Same T_c (on) value, which is also very near to the highest value of 93 K, of as-sintered and oxygenated samples indicates the similar stoichiometry of these samples. Large transition widths and differences between the transition widths of samples can be explained in terms of the presence of impurity phases and/or variations on T_c (on) values of intergrain regions, respectively. That is, post-annealing under oxygen flow seems to improve the T_c (on) values of intergrain regions.

Fig. 3b shows the M–T curves of as-sintered sample in different magnetic fields. Completed transition is observed at low magnetic fields. Increase of magnetic field (@500 Oe) causes no completion of transition even down to 50 K. Trapped field, on the other hand, increases with applied field. In order to understand the effects of calcination temperature, the samples were calcined at different temperatures. In Fig. 3c, field-cooled (fc) and zero-field-cooled (zfc) curves of as-sintered samples calcined at 920 and 950 °C are seen. It is clear that calcination at 950 °C reveals higher T_c (on) value, lower transition width and higher trapped field.

Fig. 4 shows the magnetization and critical current density J_c curves of as-sintered and oxygenated samples as a function of magnetic field at 10 and 77 K. The M–H curves reveal that oxygenation has no important influence on the hysteresis width. As it is seen from Fig. 4a, magnetization loop is of almost constant width above 1 T. At 77 K, magnetization seems quite sensitive to the applied field especially at low field regions in both as-sintered and oxygenated samples. However, it is interesting to note that the oxygenated sample is more sensitive to the applied field than the as-sintered one. For instance, magnetization of the oxygenated sample changes 72% in magnitude and that of the as-sintered one change 60% in magnitude with the applied field of 200 Oe. So, these materials may be

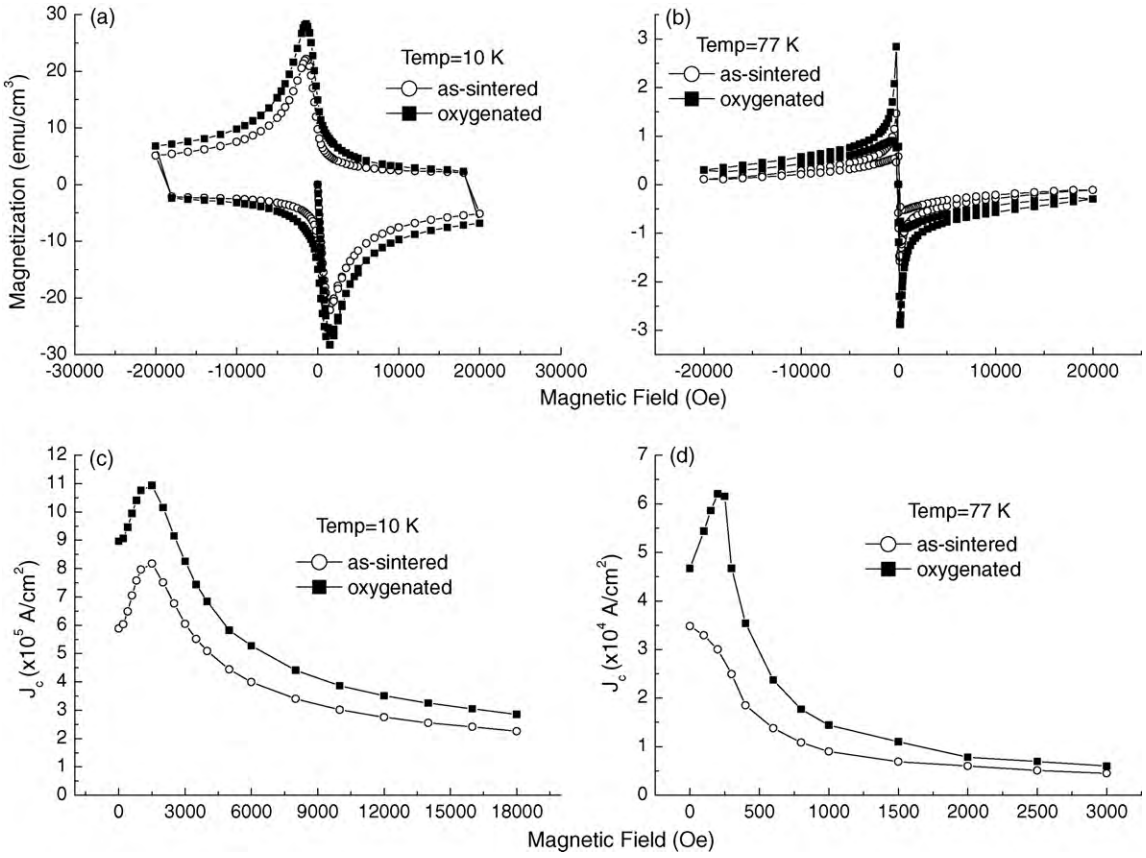

Fig. 4. (a and b) The M–H and (c and d) the J_c–H curves of as-sintered and oxygenated samples at 10 and 77 K.

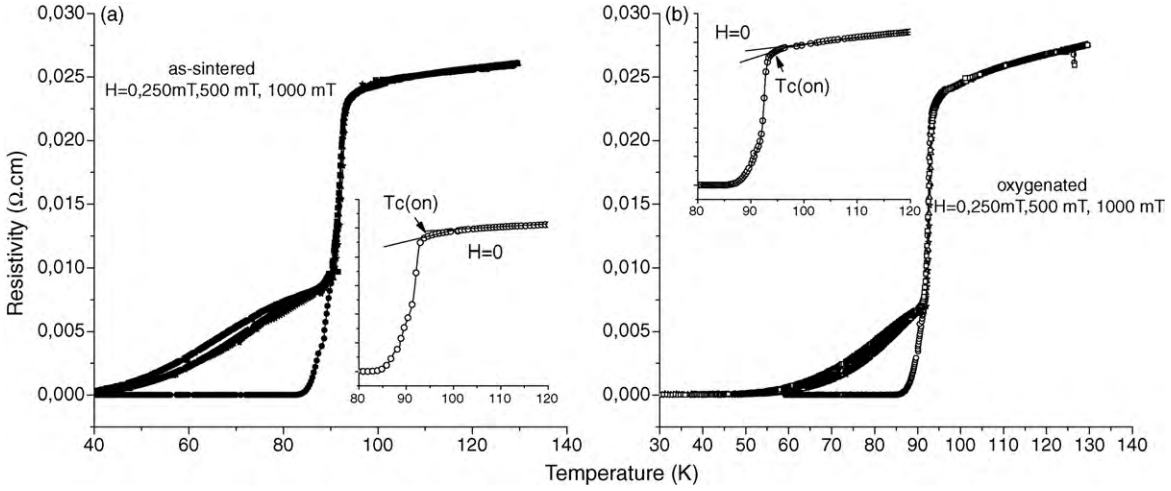

Fig. 5. The resistivity vs. temperature curves of as-sintered and oxygenated samples for different magnetic fields.

used as magnetic field sensor for the detection of ultra-low fields [17,18].

Intragrain critical current densities were determined from the M–H loops by using the Bean model [19], $J_c = 20\Delta M/d$, where d is the grain size and is taken as 10 μm. The J_c–B curves reveal a maximum on J_c values at low field regime (Fig. 4c–d). Actually, these maximums are just above the lower critical fields (see Ref. [20] for the H_{c1} values of Y-123). With the increase of temperature, the field at which the maximums are seen takes lower values. Previous studies have shown that such types of maximum points are seen on the melt-textured RE-123 (RE = Sm, Nd, Y, etc.) superconductors [21] and the J_c–T curves of granular structures in which J_c was calculated from transport measurements [22]. Besides, as seen from Fig. 4c–d, oxygenation improves the J_c values considerably. This improvement is especially significant at low fields and temperatures. For instance, at 10 K and zero fields, J_c increases by 50% in magnitude with the oxygenation. On the other hand, it increases 30% in magnitude at 77 K and 3000 Oe. The J_c values of the as-sintered and the oxygenated samples are $\sim 8 \times 10^5$ and $\sim 1.1 \times 10^6$ A/cm^2 respectively, at 10 K. Such high J_c values are most probably due to the self-induced Y-211 phase. In addition, these values represent intragrain critical current densities. That is, intergrain critical current densities determined from electrical measurements may be lower than that of intragrain ones by 10^3–10^4 orders of magnitude in polycrystalline superconductors [23].

Fig. 5 shows the ρ–T curves of as-sintered and the oxygenated samples measured under different magnetic fields. As seen, oxygenation has no significant influence on the onset critical temperatures, T_c (on). T_c (on) was determined to be ~94.5 K for both as-sintered and the oxygenated samples, which deviates from the results of M–T measurements. The intragrain T_c (on) extracted from the M–T curves (90 K) is lower than the intergrain T_c (on) obtained from the resistivity curves. Notice that the T_c (on) values are even higher than the values reported for well-studied Y-123 phase (~93 K). On the other hand, the transition widths are large in the studied samples, but it decreases with the oxygenation. It is determined to be 10 K and 7 K for as-sintered and the oxygenated samples, respectively. Large transition widths can be associated with the high misorientation angle or weak links between grains [24–25]. Same T_c (on) values together with different transition widths indicates that oxygenation is effective on the grain boundaries. That is, volume fraction of lower T_c phase between grains decreases with oxygenation. It is also apparent from the magnetic field dependence of the ρ–T curves. Superconducting transition continues down to 40 K in as-sintered sample under field of 1 T (see Fig. 5a). With oxygenation, the transition is seen as completed at 60 K under same field. Another characteristic behavior of the studied samples is a significant branching seen on the ρ–T curves with magnetic field, which is observed at temperatures much lower than T_c (on). This branching is seen at 90.5 and 91.5 K for as-sintered and oxygenated samples, respectively. The T_c (on) values and normal state resistivity are independent of the applied field. Besides, the ρ–T curves reveal the metallic character of the samples at temperature above T_c (on). The $d\rho/dT$ is determined to be 0.05 mΩ cm/K and 0.1 mΩ cm/K for as-sintered and the oxygenated samples, respectively. The value of $d\rho/dT$ increases considerably below ~100 K in both samples, which has not been observed in other cuprate superconductors. It seems to be peculiar to the studied samples.

4. Conclusion

Our experiments have shown that synthesis of Y–Ba–Cu–O superconductors with initial mixtures of Y_2O_3, $BaCO_3$ and CuO powders at nominal composition of $YBaCu_2O_x$ requires no further annealing under oxygen flow in order to get acceptable superconducting properties. Annealing under oxygen flow was observed to be not effective on superconducting transition temperature T_c (on), which was determined from magnetic and electrical measurements. Magnetic measurements reveal that both as-sintered and oxygenated samples show transition to the superconducting state at 90 K. On the other hand, electrical measurements reveal that superconducting transition starts at 94.5 K in both samples. The reason of such difference on T_c (on) values may be low concentration of superconducting carriers down to 90 K, which has not significant contribution to overall magnetization. It is also extracted from these measurements that density of superconducting charge carriers, which determines T_c (on), are same in as-sintered and oxygenated samples. It was observed that oxygenation improves the superconducting properties of intergrain regions but it has no important contribution to superconductivity of intragrain regions in the studied samples.

Acknowledgements

We would like to thank Mr. Mehmet Celik and Dr. Muharrem Asar for previewing the article and for their valuable suggestions.

References

[1] D.E. Morris, J.H. Nickel, J.Y.T. Wei, N.G. Asmar, J.S. Scott, U.M. Scheven, C.T. Hultgren, A.G. Markelz, J.E. Post, P.J. Heaney, D.R. Veblen, R.M. Hazen, Phys. Rev. B Vol.39 (1989) 7347.
[2] J.L. Tallon, D.M. Pooke, R.G. Buckley, M.R. Presland, F.J. Blunt, Phys. Rev. B 41 (1990) 7220.
[3] T. Graf, G. Triscone, J. Muller, J. Less, Common Met. 159 (1990) 349.
[4] X. Yao, T. Mizukoshi, M. Egami, H. Zama, M. Nakamura, Y. Shiohara, Jpn. J. Appl. Phys. 35 (1996) 2126.
[5] S.S.P. Parkin, E.M. Engler, V.Y. Lee, R.B. Beyers, Phys. Rev. B 37 (1988) 131.
[6] K. Przybylski, T. Brylewski, M. Bucko, J. Therm. Anal. 45 (1995) 1099.
[7] T. Shigematsu, N. Nakanishi, Solid State Ionics 40/41 (1990) 799.
[8] S. Anand, O.N. Srivastava, Bull. Mater. Sci. 27 (2004) 113.
[9] N. Chikumoto, T. Machi, Y. Tokunaga, T. Izumi, S. Tajima, Physica C 426–431 (2005) 1118.
[10] U. Balachandran, R.B. Poeppel, J.E. Emerson, S.A. Johnson, M.T. Lanagan, C.A. Youngdahl, D. Shi, K.C. Goretta, N.G. Eror, Mater. Lett. 61 (2007) 2859.
[11] D.M. Pooke, R.G. Buckley, M.R. Presland, J.L. Tallon, Phys. Rev. B 41 (1990) 6616.
[12] U. Topal, H. Sozeri, H. Yavuz, Physica C 408–410 (2004) 636.
[13] M. Murakami, et al., Physica C 185–189 (1991) 321.
[14] M. Murakami, Melt Processed High-Temperature Superconductors, World Scientific Publishing Co., Pte., Ltd., 1992, ISBN 981-02r-r1244-5.
[15] G. Iadonisi, V. Cataudella, D. Ninno, M.L. Chiofalo, Phys. Lett. A 196 (1995) 359.
[16] K.V. Ramanujachary, S. Li, M. Greenblatt, Physica C 165 (1990) 377.
[17] M. Gershenson, IEEE Trans. Magn. 27 (1991) 3055.
[18] J.C. Gallop, S. Lilleyman, C.D. Langham, W.J. Radcliffe, M. Stewart, IEEE Trans. Magn. 25 (1989) 896.
[19] J.C. Bean, Phys. Rev. Lett. 8 (1962) 250.
[20] D.-X. Chen, R.B. Goldfarb, R.W. Cross, A. Sanchez, Phys. Rev. B 48 (1993) 6426.
[21] U. Topal, L. Dorosinskii, H. Sozeri, Physica C 407 (2004) 49.
[22] H. Hilgenkamp, J. Mannhart, Rev. Mod. Phys. 74 (2002) 485.
[23] U. Topal, M.E. Yakinci, Mater. Chem. Phys. 119 (2010) 182.
[24] D.A. Cardwell, A.D. Bradley, N.H. Babu, M. Kambara, W. Lo, Supercond. Sci. Technol. 15 (2002) 639.
[25] Ph. Vanderdemden, A.D. Bradley, R.A. Doyle, W. Lo, D.M. Astill, D.A. Cardwell, A.M. Campbell, Physica C 302 (1998) 257.